Arabidopsis PAD4 lipase-like domain is a minimal functional unit in resistance to green peach aphid

Joram A. Dongus[1], Deepak D. Bhandari[1%], Monika Patel[2], Lani Archer[2], Lucas Dijkgraaf[1,3], Laurent Deslandes[4], Jyoti Shah[2] and Jane E. Parker[1*]

[1] - Department of Plant-Microbe Interactions, Max Planck Institute for Plant Breeding Research, Carl-von-Linné-weg 10; 50829 Cologne, Germany.

[2] - Department of Biological Sciences, University of North Texas; 1511 West Sycamore, Denton, Texas 76201, U.S.A.

[3] – Plant-Microbe Interactions - Utrecht University, Padualaan 8; 3584 CH Utrecht, Netherlands.

[4] – LIPM, Université de Toulouse, INRA, CNRS, Castanet-Tolosan, France

% - present address: Plant Research Laboratory, Michigan State University, USA

*Corresponding author: Jane E. Parker: parker@mpipz.mpg.de

Keywords: PAD4, EDS1, plant, basal immunity, ETI, aphid.

Funding: This work was supported by the Max Planck Society and Deutsche Forschungsgemeinschaft (DFG) Grants: DFG-ANR Trilateral ‘RADAR’ grant (JAD, LaD (ANR-15-CE20-0016-01), JEP), CRC670 (DDB, JEP), and MP was supported by a scholarship from the University of North Texas.

Abstract

Plants have evolved mechanisms to attract beneficial microbes and insects while protecting themselves against pathogenic microbes and pests. In Arabidopsis, the immune regulator PAD4 functions with its cognate partner EDS1 to limit pathogen growth. PAD4, independently of EDS1, reduces infestation by Green Peach Aphid (GPA). How PAD4 regulates these defense outputs is unclear. By expressing the N-terminal PAD4-lipase-like domain (LLD) without its C-terminal 'EDS1-PAD4' (EP) domain, we interrogated PAD4 functions in plant defense. Here we show that transgenic expression of $PAD4^{LLD}$ in Arabidopsis is sufficient for limiting GPA infestation, but not for conferring basal and effector-triggered pathogen immunity. This suggests that the C-terminal PAD4-EP domain is necessary for EDS1-dependent immune functions. Moreover, $PAD4^{LLD}$ is not sufficient to interact with EDS1, indicating the PAD4-EP domain is required for heterodimerisation. These data provide molecular evidence that PAD4 has domain specific functions.

Keywords: PAD4, EDS1, plant, basal immunity, ETI, aphid.

Introduction

To colonize plants, pathogenic microbes and pests (such as aphids or nematodes) deliver susceptibility factors, called effectors, to the host which target defenses and reprogram cells to promote infection or infestation. Many host-adapted biotrophic and hemi-biotrophic pathogens deploy effectors to disable PAMP/MAMP-triggered immunity (PTI) mediated by cell surface-resident receptors [Boutrot & Zipfel, 2017; Dangl & Jones, 2006; Dodds & Rathjen, 2010]. These microbes encounter two further important immunity barriers. One is conferred by intracellular nucleotide-binding leucine-rich repeat (NLR) receptors recognizing interference by specific effectors [Jones et al., 2016]. NLR activation leads to effector-triggered immunity (ETI) involving the rapid transcriptional mobilization of resistance pathways and, often, localized host cell death, which limit pathogen infection [Bhandari et al., 2019; Cui et al., 2015; Mine et al., 2017]. NLR-mediated immune responses are also effective against probing insects and nematodes [Milligan et al., 1998; Rossi et al., 1998; Villada et al., 2009; Wroblewski et al., 2007]. A second barrier, called basal immunity, slows virulent pathogen growth and disease progression by eliciting a weak immune response [Cui et al., 2015; Cui et al., 2017; Dangl & Jones, 2006]. Although the precise activation mechanism for post-infection basal immunity is not known, in Arabidopsis it requires several ETI signaling components [Century et al., 1995; Feys et al., 2001; Glazebrook et al., 1997; Parker et al., 1996], and is proposed to be the culmination of weak NLR-triggered ETI combined with residual PTI [Cui et al., 2017; Gantner et al., 2019].

In Arabidopsis, the nucleocytoplasmic immune regulator PAD4 (PHYTOALEXIN DEFICIENT4) signals in both ETI and basal immunity by stimulating production of the defense hormone salicylic acid (SA) and anti-microbial molecules, which limit pathogen growth [Glazebrook et al., 1997; Jirage et al., 1999; Wiermer et al., 2005; Zhou et al., 1998]. PAD4 is a member of a small family (the EDS1 family) of sequence-related

immunity regulators, comprising also EDS1 (ENHANCED DISEASE SUSCEPTIBILITY1) and SAG101 (SENESCENCE ASSOCIATED GENE101) [Feys et al., 2005; Lapin et al., 2019]. Arabidopsis EDS1 and PAD4 function together in conferring ETI governed by a sub-class of NLRs with N-terminal Toll-interleukin1 Receptor domains (known as TIR-NLRs or TNLs) [Feys et al., 2005; Jones et al., 2016; Wagner et al., 2013]. Genetic and molecular studies in Arabidopsis revealed that activated TNL receptors stimulate EDS1-PAD4 basal immunity activity to transcriptionally boost SA signaling and other defense responses, and repress antagonistic jasmonic acid (JA) hormone pathways [Cui et al., 2017; Cui et al., 2018]. In Arabidopsis, the EDS1-PAD4 transcriptional reprogramming function in pathogen immunity requires a nuclear EDS1 pool [Bartsch et al., 2006; Cui et al., 2017; Garcia et al., 2009; Stuttmann et al., 2016].

EDS1, PAD4 and SAG101 each possess an N-terminal lipase-like domain (LLD) with an α/β hydrolase topology resembling eukaryotic class-3 lipase enzymes [Rauwerdink & Kazlauskas, 2015; Wagner et al., 2013; Wang et al., 2018], and a structurally unique C-terminal EP (EDS1-PAD4) domain consisting of α-helical bundles [PFAM database: PF18117; Wagner et al., 2013]. The EDS1 and PAD4, but not SAG101, LLDs have a canonical Ser-Asp-His (S-D-H) catalytic triad that is characteristic for α/β hydrolases [Wagner et al., 2013]. The serine is part of a characteristic lipase GXSXG motif which is conserved in EDS1 and PAD4 proteins across seed plant (angiosperm and gymnosperm) species [Wagner et al., 2013; Lapin et al., 2019]. Strikingly, the S-D-H residues were found to be dispensable for EDS1 and PAD4 signaling in Arabidopsis TNL-mediated ETI and basal immunity, indicative of a non-catalytic mechanism in pathogen resistance [Louis et al., 2012; Wagner et al., 2013].

EDS1 forms stable and mutually exclusive heterodimers with PAD4 or SAG101, consistent with distinct roles of these two EDS1 complexes in immunity [Lapin et al., 2019; Rietz et al., 2011; Wagner et al., 2013]. Based on a structural model of the EDS1-PAD4 heterodimer generated from the *At*EDS1-*At*SAG101 crystal structure, analysis showed that the juxtaposed LLDs are major drivers of heterodimerisation, likely promoting association of the aligned EP domains to form a cavity [Wagner et al., 2013]. The *At*EDS1^{LLD} alone, although stable, did not confer pathogen resistance, indicating that its EP domain is crucial for immune signaling activity [Wagner et al., 2013]. Further structure-based analysis identified an *At*EDS1 EP-domain surface lining the EDS1-PAD4 heterodimer cavity which is essential for the rapid transcriptional reprogramming of host cells in Arabidopsis TNL ETI [Bhandari et al., 2019; Lapin et al., 2019].

In Arabidopsis, *PAD4* mediates resistance to green peach aphid (GPA, *Myzus persicae* Sülzer) independently of *EDS1* and *SAG101* [Pegadaraju et al., 2005 & 2007]. GPA population growth was higher on Arabidopsis *pad4* compared to wild-type (WT) and *eds1*, *sag101* or *eds1/sag101* mutant plants [Pegadaraju et al., 2007]. Notably, *PAD4*-mediated defenses against GPA were found to not involve SA or camalexin production [Pegadaraju et al., 2005]. Moreover, in contrast to basal immunity and ETI, resistance to GPA was dependent on the S-D-H predicted catalytic triad residues PAD4^{S118} and PAD4^{D178}, but not PAD4^{H229} [Louis et al., 2012; Wagner et al., 2013]. These different requirements suggest that PAD4 functions in immunity as a heterodimer with EDS1 are distinct from its function in resistance to GPA.

To gain a deeper insight into the molecular function of PAD4, we investigate here the properties of the PAD4^{LLD} in resistance to GPA and pathogen immunity. We show that the PAD4^{LLD} alone is sufficient to control GPA infestation, independently of EDS1 association. By contrast, we find that the Arabidopsis PAD4^{LLD} is insufficient for EDS1-

dependent basal immunity and ETI, indicating that, like EDS1, the PAD4 EP domain is crucial for inducing immunity pathways. These results suggest that PAD4 can operate as a bipartite protein with the LLD and EP domains carrying out distinctive and separable roles in plant defense.

Results

The PAD4^{LLD} protein accumulates *in planta,* but does not interact with EDS1

*At*EDS1-*At*PAD4 heterodimer formation is driven chiefly by an N-terminal EDS1 hydrophobic loop (α-helix H; EDS1^{LLIF}) and the juxtaposed PAD4^{MLF} motif (Figure 1A-C) [Feys et al*.,* 2001; Wagner et al*.,* 2013]. To test PAD4^{LLD} properties, we generated an *At*PAD4^{LLD} protein (residues 1-299; Figure 1A; blue). Transient overexpression of GFP-tagged PAD4^{LLD} in *Nicotiana benthamiana* produced a stable protein that did not co-immunoprecipitate (co-IP) FLAG-tagged EDS1, whereas full-length GFP-PAD4 did (Figure 1D). Similarly, PAD4^{LLD} failed to interact with EDS1 in an *N. benthamiana* split-luciferase assay (Figure S1). These data suggest that a stable interaction between PAD4 and EDS1 *in planta* requires part or all of the PAD4 EP domain in addition to the LLD interface.

To investigate PAD4^{LLD} properties in Arabidopsis, we introduced WT PAD4 (*pPAD4*::s*trepII-YFP-cPAD4^{WT}*) or PAD4^{LLD} (*pPAD4*::s*trepII-YFP-cPAD4^{LLD}*) constructs into a *pad4-1/sag101-3* mutant (Col-0 accession). PAD4^{LLD} in two independent stable transgenic lines showed a nucleocytoplasmic localization similar to PAD^{WT} at 24 h post infection (hpi) with *Pseudomonas syringae* pv. *tomato* strain DC3000 expressing the effector avrRps4 (*Pst avrRps4*) (Figure S2). Delivery of avrRps4 by *Pst* triggers ETI in Col-0 mediated by the receptor pair RRS1-S/RPS4 (RESISTANCE TO RALSTONIA SOLANACEARUM1-S/RESISTANCE TO PSEUDOMONAS SYRINGAE4) [Birker et al*.,* 2009*;* Heidrich et al*.,* 2011; Narusaka et

al., 2009; Saucet et al., 2015]. The PAD4^{LLD} distribution is in line with previously described nucleocytoplasmic localizations of EDS1^{LLD} and PAD4^{LLD}/SAG101$^{EP\ domain}$ chimeras *in planta* [Lapin et al., 2019; Wagner et al., 2013]. PAD4^{LLD} protein was also immuno-detected from leaf samples treated with *Pst avrRps4*, although at much lower levels compared to PAD4^{WT} lines (Figure 1E). This contrasts with similar PAD4^{LLD} and PAD4^{WT} accumulation in *N. benthamiana* transient assays (Figure 1D). Lower PAD4^{LLD} protein accumulation than PAD4^{WT} in mock- and *Pst avrRps4*-treated Arabidopsis leaves can be attributed in part to lower accumulation of *PAD4* transcripts in the PAD4^{LLD} compared to PAD4^{WT} transgenic lines (Figure 1F). Hence, the LLD domain of PAD4 is sufficient to maintain a WT-like nucleocytoplasmic localization, but loss of the EP domain substantially reduces PAD4-EDS1 interaction and PAD4 steady-state levels in Arabidopsis.

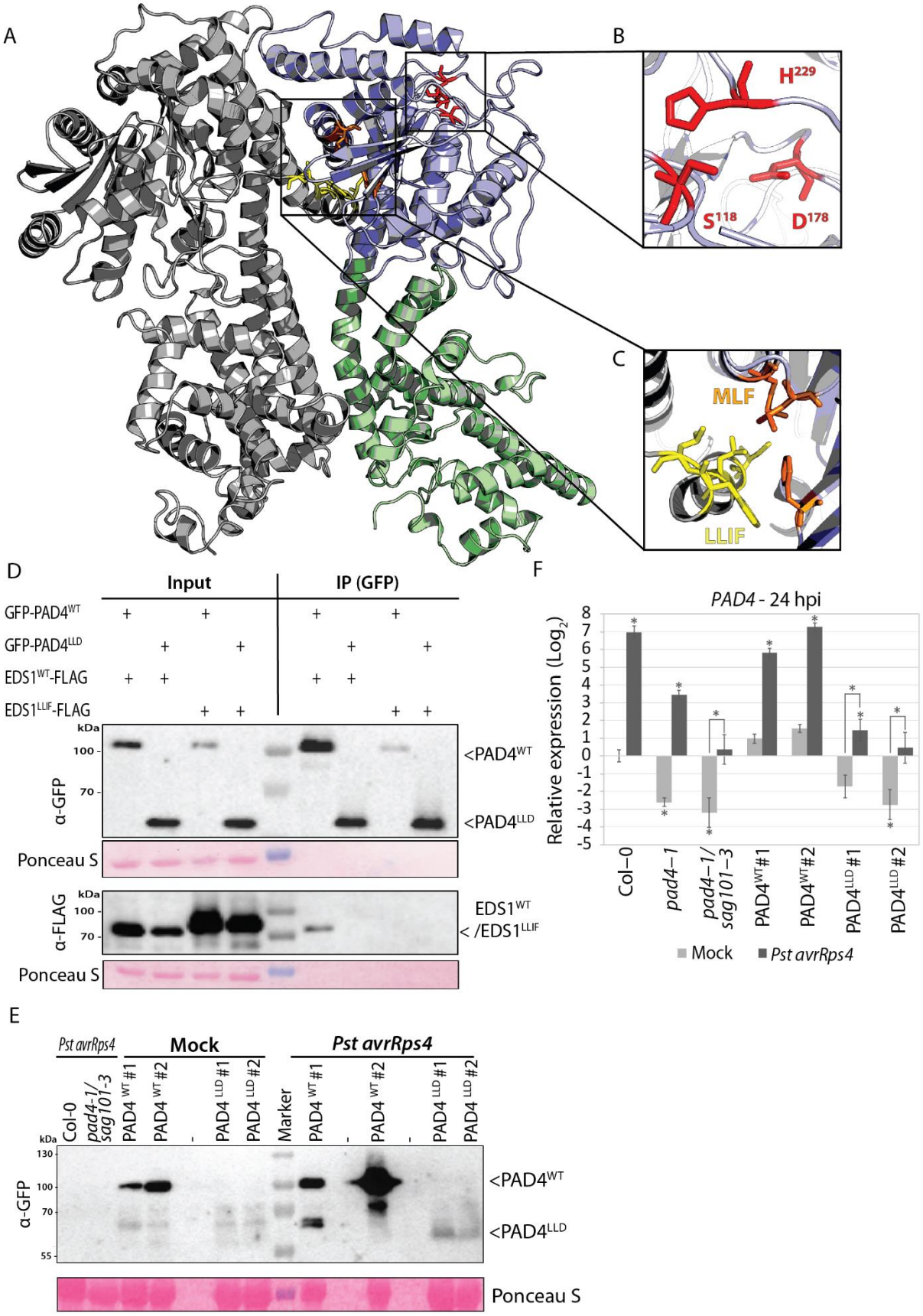

Figure 1. PAD4^{LLD} accumulates *in planta* but does not interact with EDS1

A. EDS1-PAD4 heterodimer model, based on the *At*EDS1-*At*SAG101 crystal structure [Wagner et al*.,* 2013]. EDS1 (Grey), PAD4 (LLD) (blue) and PAD4 EP domain (green) are represented in cartoon format.

B. PAD4 catalytic triad residues S^{118}, D^{178} and H^{229} in the LLD are shown as red sticks.

C. EDS1-PAD4-interacting motifs EDS1^{LLIF} and PAD4^{MLF} are colored with yellow and orange sticks, respectively.

D. Co-immunoprecipitation (GFP-trap) of GFP-PAD4/PAD4^{LLD} with EDS1/EDS1^{LLIF}-3xFLAG transiently expressed in *N. benthamiana* leaves (using *35S::GFP-PAD4/PAD4^{LLD}* and *35S::EDS1/EDS1^{LLIF}-3xFLAG* constructs, respectively) A representative image from three independent experiments is shown.

E. PAD4 accumulation in independent stable transgenic Arabidopsis lines expressing YFP-PAD4^{WT} and YFP- PAD4^{LLD} probed by Western blotting using α-GFP antibody at 24 hpi with mock (10 mM $MgCl_2$) or *Pst* AvrRps4 treatments. A representative image from three independent experiments is shown.

F. *PAD4* transcript abundance was determined by RT-qPCR at 24 hpi in mock- or *Pst* AvrRps4-treated samples of the indicated Arabidopsis lines. Data are pooled from three independent experiments each with two to three biological replicates (n = 6-9). Bars represent means of three experimental replicates ± SE. Relative expression and significance level is set to Col-0 mock-treated samples. Asterisk indicates $p < 0.01$, one-way ANOVA with multiple testing correction using Tukey-HSD.

Expression of PAD4^{LLD} confers GPA resistance

PAD4 acts independently of EDS1 to restrict aphid infestation, and this function is dependent on the PAD4^{LLD} located S^{118} and D^{178} predicted α/β-hydrolase catalytic triad residues (Figure 1A & 1B) [Louis et al*.,* 2012; Pegadaraju 2007]. Since PAD4^{LLD} accumulates in Arabidopsis, we tested whether the PAD4^{LLD} alone is able to resist GPA infestation. Consistent with earlier data [Louis et al*.,* 2012; Pegadaraju et al*.,* 2007], *pad4-1, pad4-1/sag101-3* and a PAD4^{S118A} line (in *pad4-1/eds1-2/EDS1^{SDH};* Wagner et al*.,* 2013) permitted a significant increase in aphid population size compared to Col-0 in a no-choice bioassay, indicating compromised resistance to GPA infestation (Figure 2). The PAD4^{LLD} lines resisted GPA to similar levels as PAD4^{WT} and Col-0, even though they expressed very low PAD4^{LLD} amounts (Figure 2). Hence, low steady state accumulation of PAD4^{LLD} protein (Figure 1E) is sufficient to counter GPA infestation in

185 Arabidopsis, implying that PAD4^{LLD} has an *in planta* activity. Based on these data we
186 conclude that PAD4^{LLD} is a stable protein entity able to confer GPA resistance.

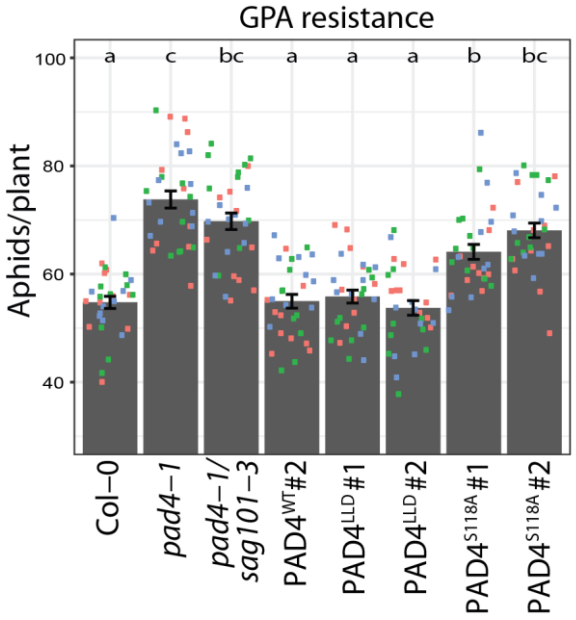

187

188 **Figure 2. PAD4^{LLD} is sufficient for GPA resistance**
189 Numbers of green peach aphids (GPA) per plant at 11 days post-infestation in a no-
190 choice assay. Data are pooled from three independent experiments each with ten
191 biological replicates per experiment (n = 30). Squares of the same color represent ten
192 biological replicates in an independent experiment. Bars represent mean of three
193 experimental replicates ± SE. Differences between genotypes were determined using
194 ANOVA (Tukey-HSD, p <0.01), letters indicate significance class.

195

196 **Arabidopsis ETI and basal pathogen immunity require full-length PAD4**

197 Since PAD4^{LLD} transgenic plants were as resistant as Col-0 against GPA, we tested if
198 the PAD4^{LLD} domain also functions in basal and/or TNL-triggered pathogen immunity.
199 For this, we measured TNL ETI using the biotrophic pathogen *Hyaloperonospora*
200 *arabidopsidis* (*Hpa*) isolate EMWA1, which is recognized in Col-0 by the TNL *RPP4*
201 (*RESISTANCE TO PERONOSPORA PARASITICA4*) [Van der Biezen et al., 2002;
202 Asai et al., 2018]. Col-0, PAD4^{WT} and PAD4^{S118A} lines were fully resistant to *Hpa*
203 EMWA1, as measured by conidiophore production (Figure 3A). By contrast, PAD4^{LLD}
204 transgenic lines were fully susceptible with conidiophore production and macroscopic

disease and microscopic *Hpa* colonization phenotypes resembling a *pad4-1/sag101-3* mutant (Figure 3A & Figure S3).

Further, we tested PAD4^{LLD} function in TNL (RRS1-S/RPS4) ETI to *Pst avrRps4* and in basal immunity to virulent *Pst* DC3000. In basal immunity, *pad4-1* is as susceptible as *pad4-1/sag101-3* while in ETI, *pad4-1* displays intermediate susceptibility between Col-0 and *pad4-1/sag101-3* (Figure 3B & 3C) [Feys et al., 2005; Wagner et al., 2013]. In line with published data, PAD4^{S118A} was as resistant as Col-0 and PAD4^{WT} in both basal immunity and ETI (Figure 3B & 3C), consistent with previous findings that the PAD4 S-D-H predicted catalytic triad is not required for pathogen immunity [Louis et al., 2012; Wagner et al., 2013]. PAD4^{LLD} lines were fully susceptible to *Pst* DC3000 and *Pst avrRps4*, with bacterial titers comparable to *pad4-1/sag101-3* (Figure 3B & 3C), indicating that PAD4^{LLD} is not able to confer basal immunity or ETI. Also, PAD4^{LLD} expressing plants and *pad4-1/sag101-3* failed to induce expression of defense marker genes 24 hpi with *Pst avrRps4*, indicating that PAD4^{LLD} is unable to signal in TNL ETI (Figure 3D-F & Figure S4). Taken together, the *Hpa* and *Pst* infection data show that PAD4^{LLD} is non-functional in pathogen basal immunity and ETI, in stark contrast to its resistance activity against GPA.

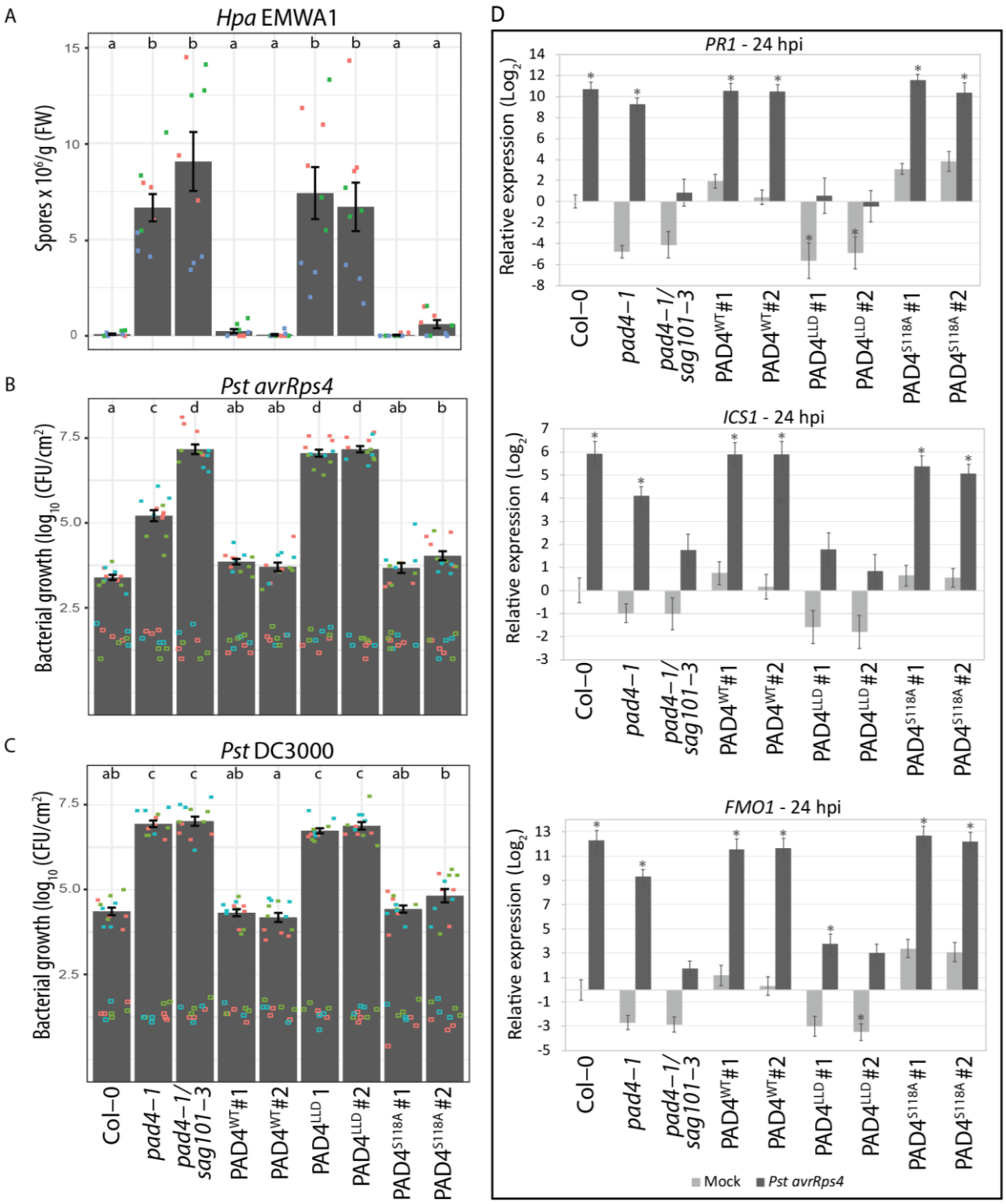

Figure 3. PAD4^{LLD} is not functional in Arabidopsis ETI and basal immunity

A. TNL (RPP4) ETI assay in Arabidopsis independent transgenic lines with wild-type and mutant controls, as indicated. *Hpa* EMWA1 conidiospores on leaves were quantified at 6 dpi in three independent experiments (squares; n=9). Col-0 (resistant), *pad4*-1 (susceptible) and *pad4-1/sag101-3* (susceptible) functioned as controls. Squares of the same color represent three biological replicates in an independent experiment. Bars represent mean of three experimental replicates ± SE. Differences between genotypes were determined using ANOVA (Tukey-HSD, p <0.01), letters indicate significance class.

B. TNL (RRS1-S/RPS4) ETI assay in the same Arabidopsis independent transgenic and control lines as in A. Four-week old Arabidopsis plants were syringe infiltrated with *Pst avrRps4* (OD_{600} = 0.0005) and bacterial titers were determined at 0 dpi (empty squares; n=8-9) and 3 dpi (filled squares; n=11-12). Squares of the same color represent 2-3 (day 0) or 3-4 (day 3) biological replicates in an independent experiment. Bars represent mean of three experimental replicates ± SE. Differences between genotypes were determined using ANOVA (Tukey-HSD, p <0.01), letters indicate significance class.

C. Infection assay was performed with basal immunity triggering *Pst* DC3000 (OD_{600} = 0.0005). Experimental set-up and statistical analysis as in B.

D. Transcript abundance determined by RT-qPCR in 4-week old Arabidopsis plants syringe-infiltrated with either buffer (mock, grey bars) or *Pst avrRps4* (black bars) (24 hpi). Data are pooled from three independent experiments, with two to three biological replicates per experiment (n = 6-9). *PATHOGENESIS RELATED1* (*PR1*), *ISOCHORISMATE SYNTHASE1* (*ICS1*), and *FLAVIN MONOOXYGENASE1* (*FMO1*) transcript abundances were measured relative to *ACTIN2* (*ACT2*). Relative expression and significance level is set to Col-0 mock-treated samples. Differences between genotypes were determined using ANOVA (Tukey-HSD), asterisks indicate p < 0.01.

Discussion

PAD4 controls Arabidopsis defenses against pathogens and aphids, playing major roles with EDS1 in basal and effector-triggered immunity, and an *EDS1*-independent role in resistance to GPA [Bhandari et al., 2019; Cui et al., 2017; Cui et al., 2018; Glazebrook et al., 1997; Lapin et al., 2019; Louis et al., 2012; Pegadaraju et al., 2007; Rietz et al., 2011; Wagner et al., 2013]. In this study, we investigated the contribution of the PAD4^{LLD} to these different defense outputs. Analysis of PAD4^{LLD} *in planta* shows that it accumulates to much lower levels than full-length PAD4 and has lost binding to EDS1. Strikingly, PAD4^{LLD} confers complete GPA resistance (Figure 2), but is non-functional in resistance to *Hpa* and *Pst* pathogens (Figure 3). Thus, PAD4 appears to rely solely on its LLD for controlling GPA infestation, whereas its LLD and EP domains are necessary for ETI and basal immunity against bacterial and oomycete pathogens. These data suggest there are domain specific signaling functions of Arabidopsis PAD4.

Recent studies suggest that the N-terminal LLDs of Arabidopsis EDS1 and PAD4 act as a scaffold, enabling the C-terminal EP domains to interact and orchestrate

downstream immune signaling as a heterodimer [Bhandari et al., 2019; Lapin et al., 2019; Wagner et al., 2013]. By testing the PAD4^{LLD} without its EP domain, our data show that PAD4, like EDS1 [Bhandari et al., 2019], requires its EP domain for immunity signaling. By contrast, the PAD4^{LLD} is sufficient to limit GPA proliferation, thus highlighting a role of the PAD4^{LLD} and its α/β-hydrolase catalytic triad as a minimal functional unit in GPA resistance. *At*EDS1 and *At*PAD4 proteins mutually stabilize each other [Feys et al., 2001; Feys et al., 2005; Rietz et al., 2011; Wagner et al., 2013]. The fact that interaction between PAD4^{LLD} and EDS1 is greatly diminished compared to interaction between full-length PAD4 and EDS1 (Figure 1D), tallies with the observation that *PAD4*-dependent GPA resistance is independent of *EDS1* [Pegadaraju et al., 2007].

The PAD4^{LLD} adopts an α/β hydrolase fold with a core S-D-H predicted catalytic triad. The α/β hydrolase family catalyzes a variety of enzymatic reactions such as esterification, hydrolysis and acyl transfer [Rauwerdink & Kazlauskas, 2015]. The S-D-H predicted catalytic triad of PAD4 is dispensable for immune signaling against *Hpa* and *Pst*, but required for GPA resistance [Louis et al., 2012; Wagner et al., 2013]. In the *At*PAD4 structural model, this triad of residues is solvent-accessible (Figure 1A & 1B), suggesting a plausible catalytic function. However, this applies only to Brassicaceae PAD4 proteins, as beyond the Brassicaceae clade PAD4 contains an insertion, which forms a “lid” covering the S-D-H triad similar to that in *At*EDS1, rendering it inaccessible to the solvent [Wagner et al., 2013]. Such helical loop structures extending from the β-sheet scaffold have been found to regulate the enzymatic activity of inactive-state triacylglycerol lipases [Khan et al., 2017]. Hence, it is possible that the PAD4 S-D-H triad functions differently outside the Brassicaceae clade [Wagner et al., 2013]. Critically, all three residues in the catalytic triad are

required for hydrolase activity [Rauwerdink & Kazlauskas, 2015]. Since loss of H^{229} does not affect *At*PAD4-mediated deterrence of GPA [Louis et al., 2012], it is more likely that PAD4 involvement in Arabidopsis defense against the GPA does not rely on a canonical hydrolase activity.

Alternatively, the S-D-H triad in PAD4 could function as a receptor ligand-binding domain, a common feature of α/β hydrolase fold proteins [Mindrebo et al., 2016]. For example, the Arabidopsis karrikin receptor *At*KAI2 (KARRIKIN INSENSITIVE 2) uses its catalytically inactive S-D-H triad for ligand recognition [Guo et al., 2013]. Catalytically inactive rice (*Os*) and *At*GID1 (GIBBERELLIN (GA) INSENSITIVE DWARF1) uses a modified triad (S-D-V) to bind bioactive GA molecules, indicating that the histidine, which is required for catalytic activity, can be replaced by another residue for functional ligand binding [Murase et al., 2008; Rauwerdink & Kazlauskas, 2015; Shimada et al., 2008]. Upon binding to GA, a conformational change in *At*GID1 results in the assembly of a SCF^{GID1} (SKP-Cullin-F-box^{GID1}) complex and ubiquitination of DELLA proteins marking them for proteasome-mediated degradation [Murase et al., 2008]. Together with the data presented here, these examples highlight the possibility that the $PAD4^{LLD}$ domain serves as a ligand-binding surface in a protein signaling complex, rather than a lipase.

The inactivity of $PAD4^{LLD}$ in basal and effector-triggered immunity is unlikely to be attributed to $PAD4^{LLD}$ instability, as it is sufficient for resistance against GPA, unless the $PAD4^{LLD}$ fails to reach sufficient amounts needed for pathogen resistance in certain cells or tissues. Very low levels of protein were sufficient for EDS1 function in pathogen immunity [Bhandari et al., 2019; Suttmann et al., 2016; Wagner et al., 2013], and we presume this is also the case for PAD4, since EDS1 and PAD4 are functional as a heterodimer. A more plausible explanation for the susceptibility of $PAD4^{LLD}$ might be

(i) its inability to form a heterodimer with EDS1 (Figure 1A & 1D; Wagner et al., 2013) and (ii) the lack of an EP domain. Both are essential in EDS1 for immunity to *Pst* and *Hpa* infection and for rapid transcriptional up-regulation of defense genes in ETI against *Pst avrRps4* [Bhandari et al., 2019; Lapin et al., 2019; Wagner et al., 2013]. The EDS1 EP domain interface lining a cavity formed with PAD4 in the heterodimer is necessary for Arabidopsis EDS1 signaling [Bhandari et al., 2019; Lapin et al., 2019]. An aligned EP domain α-helix was identified in the EDS1 heterodimer partner, SAG101, as being essential for eliciting host cell death in TNL ETI responses [Gantner et al., 2019; Lapin et al., 2019]. This also might be true for PAD4, because mutations at an EDS1-like surface in PAD4 lying outside the cavity did not compromise immunity [Bhandari et al., 2019]. Future studies will test whether the PAD4 EP domain surface lining the heterodimer cavity is also crucial for EDS1-PAD4 pathogen immunity.

Our analysis of the LLD of Arabidopsis PAD4 demonstrates a domain-specific partitioning of defense functions - with the PAD4^{LLD} being necessary and sufficient for limiting GPA infestation, and the EP domain (with the LLD) mediating immunity signaling against *Pst* and *Hpa* (Figure 4). While the two PAD4 domains clearly have distinct roles, instability and inactivity of the PAD4 EP domain without the LLD makes it difficult to assess whether PAD4 is a bipartite immune regulator or moonlighting in GPA resistance. This study of the PAD4^{LLD} paves way for molecular dissection of the diverse roles of PAD4 in biotic stress resistance.

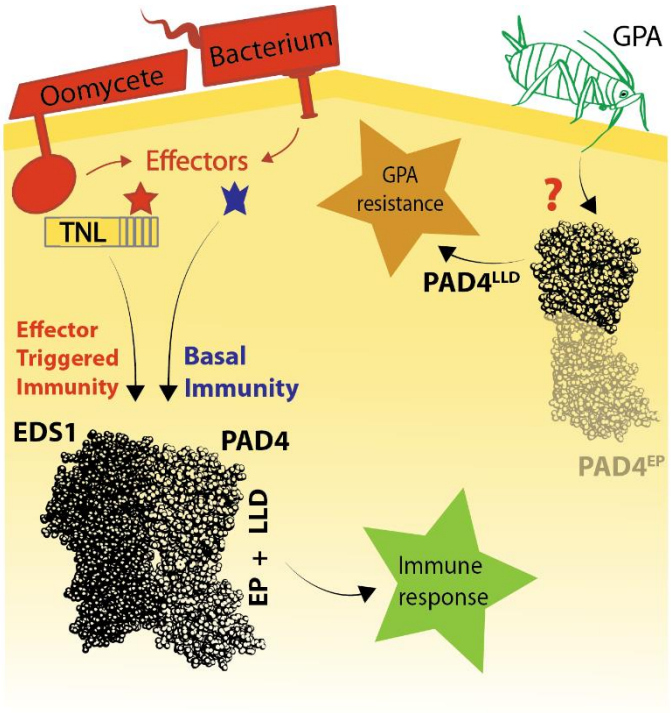

340

341 **Figure 4. Domain-specific roles of Arabidopsis PAD4 in immunity**
342 Schematic showing separable activities of PAD4^{LLD} and PAD4^{LLD} + EP domain. Upon
343 infection by bacteria or oomycetes, the EDS1-PAD4 heterodimer is activated via TNLs
344 in ETI or by other signals in basal immunity, leading to a pathogen immune response.
345 PAD4 requires both the LLD and EP domains to function in basal immunity and ETI. In
346 resistance to GPA, PAD4 is activated through an unknown but *EDS1*-independent
347 mechanism that restricts aphid infestation. PAD4^{LLD} is sufficient to limit GPA
348 independently of interaction with EDS1.

349

350

351 **Author contributions**

352 JAD, DDB, JEP designed the study; JAD, LuD, MP and LA performed experiments,

353 JAD and JEP wrote the manuscript with inputs from DDB, LaD and JS; JEP, LaD and

354 JS provided funding.

355

Acknowledgments

We would like to thank Karsten Niefind for structural insights and Neysan Donnelly for help editing the manuscript.

Materials and Methods

Plant materials, growth conditions and pathogen strains

Arabidopsis *pad4-1, sag101-3,* and *eds1-2* mutants are in the Col-0 background and were previously described, as were *pEDS1:EDS1-SDH*::*pPAD4:PAD4-S118A* (in *eds1-2/pad4-1*) and *pPAD4:StrepII-YFP-PAD4* (in *pad4-1/sag101-3*) transgenic lines (See table S1 for primers) [Bhandari et al*.,* 2019; Wagner et al*.,* 2013]. *Pseudomonas syringae* pv. *tomato* (*Pst*) strain DC3000 and *Pst avrRps4* were described previously (Cui et al*.,* 2017). Plants were grown on soil in a controlled environment and insect-free chambers under a 10 h light/14 h dark regime (PAR: 100–150 µmol/m^2/s) at 22 °C and 60% relative humidity.

Pathogen infection assays

For bacterial growth assays, *Pst avrRps4* (OD_{600}=0.0005) in 10 mM $MgCl_2$ was hand-infiltrated into leaves of 4-week-old plants. Bacterial titers were measured at 3 h post-infiltration (day 0) and 3 d, as described previously (Feys et al., 2005). Each biological replicate consisted of three leaf disks from different plants and data shown in each experiment are compiled from three to four biological replicates. Statistical analysis was performed using one-way ANOVA with multiple testing correction using Tukey's HSD (*p*-value as described in figure legend).

For gene expression analysis, leaves of 4-week-old plants were hand-infiltrated with mock (10 mM $MgCl_2$) or bacteria (OD_{600}= 0.005) and samples were taken at 24 hpi. *ACT2* was used as a reference gene (See Table S1 for primers). Data shown are results from three independent experiments each with two to three biological replicates. For protein accumulation assays, leaves from 4-week-old plants were hand-infiltrated with buffer (mock, 10 mM $MgCl_2$) or bacteria (OD_{600}= 0.005) and samples harvested by pooling leaves from at least three different plants.

Hpa isolate EMWA1 was sprayed onto 2.5 week-old plants at 4 x 10^4 spores/ml dH_2O. *Hpa* infection structures and plant host cell death were visualized using lactophenol trypan blue staining (Muskett et al*.,* 2002) and imaged by light microscopy (Zeiss Axio Imager). To quantify *Hpa* sporulation on leaves, three pots with ~ 10 plants per genotype were infected and treated as a biological replicate. Plants were harvested at 6 dpi, fresh weight was determined. Conidiospores were suspended in 5 ml dH_2O and counted under a light microscope using a Neubauer counting chamber.

Aphid no-choice bioassay

For each biological replicate five one-day-old nymphs were released onto the center of a 17-day-old plant. The total number of aphids (adult + nymphs) per biological replicate were counted 11 days post infestation. Each independent experimental replicate consisted of 10 biological replicates per genotype [Nalam et al*.,* 2018].

Plasmid constructs

The pENTR/D-TOPO *PAD4* vector used for site-directed mutagenesis was cloned from cDNA and is described [Wagner et al*.,* 2013]. $PAD4^{LLD}$ was obtained by site-directed mutagenesis on pENTR/D-TOPO *PAD4* according to the QuikChangeII site-directed

mutagenesis manual (Agilent) (See Table S1 for primers). Mutated *PAD4* and *EDS1* entry clones [Bhandari et al., 2019; Wagner et al., 2013] were verified by sequencing and recombined by an LR reaction into a pAM-PAT-based binary vector backbone [Witte et al., 2004]. Split-luciferase lines were created by LR reaction between gateway-compatible split-luciferase binary vectors [Gehl et al., 2011] and *PAD4* and *EDS1* entry clones [Bhandari et al., 2019; Wagner et al., 2013].

Generation of transgenic Arabidopsis plants

Stable transgenic lines were generated by transforming a binary expression vector (containing Basta resistance) into Arabidopsis null mutant *pad4-1/sag101*-3 [Wagner et al., 2013], using *Agrobacterium*-mediated floral dipping (*Agrobacterium tumefaciens* GV3101 PMP90 RK) [Clough and Bent, 1998]. After selecting single-insert, homozygous transgenic lines, all lines were genotyped by sequencing for the presence of the correct PAD4 transgene ($PAD4^{WT}$, $PAD4^{LLD}$ or $PAD4^{S118A}$) before performing pathogen assays.

Transient expression in *N. benthamiana*

Transient expression in *N. benthamiana* was performed by co-infiltrating *Agrobacterium* cells carrying constructs at an OD_{600} of 0.4–0.6 in a 1:1 ratio. Before syringe infiltration, *A. tumefaciens* cells were incubated for 3h at 28°C in induction buffer (150 µM acetosyringone,10 mM MES pH5.6, 10 mM $MgCl_2$) and shaked at 650 rpm in an Eppendorf Thermomixer. *N. benthamiana* leaf samples were harvested at 3 dpi and snap frozen in liquid nitrogen and stored at -80°C.

Protein extraction, immunoprecipitation (IP) and Western blotting

Total leaf extracts were processed in extraction buffer (50 mM Tris pH7.5, 150 mM NaCl, 10 % (v/v) glycerol, 2 mM EDTA, 5 mM DTT, 0.1 % Triton X-100 and protease inhibitor (Roche, 1 tablet per 50 ml)). Lysates were centrifuged for 20 min, 21,000 x *g* at 4 °C. Supernatant was used as input sample (50 µl). Immunoprecipitations were conducted by incubating the input sample (1.2 mL) with 10 µl GFP TrapMA beads (Chromotek) for 3 h at 4 °C. Beads were collected using a magnetic rack and washed four times in extraction buffer. Protein or IP samples were boiled at 96 °C in 2x Laemmli buffer for 10 min. Proteins were separated by SDS-PAGE and analyzed by immunoblotting using α-GFP (Sigma Aldrich, 11814460001) or α-FLAG (Sigma Aldrich, F7425) primary antibodies and secondary antibodies coupled to Horseradish Peroxidase (HRP, Sigma Aldrich) for protein detection on blots.

Luciferase Assay

All tested co-expression constructs were transiently expressed on one leaf. Three leaf disks (0.4 cm diameter) from three independent leaves were pooled per biological replicate and processed in reporter lysis buffer (Promega; E1500, + 150 mM Tris, pH 7.5). Samples were mixed in a 1:1 ratio with substrate (Promega; E1531) and luminescence was measured. Absolute luminescence, *i.e.* absolute luciferase activity was used as a proxy for protein-protein interaction intensity.

References

1. Asai, S., Furzer, O.J., Cevik, V., Kim, D.S., Ishaque, N., Goritschnig, S., Staskawicz, B.J., Shirasu, K., Jones, J.D.G. 2018. A downy mildew effector evades recognition by polymorphism of expression and subcellular localization. Nature Communications. 9:5192.
2. Bartsch, M.,Gobbato, E., Bednarek, P., Debey, S., Schultz, J.L., Bautor, J., Parker, J.E. 2006. Salicylic Acid-Independent ENHANCED DISEASE SUSCEPTIBILITY1 Signaling in Arabidopsis Immunity and Cell Death Is Regulated by the Monooxygenase FMO1 and the Nudix Hydrolase NUDT7. Plant Cell. 18:1038-1051.
3. Boutrot, F., Zipfel, C. 2017. Function, Discovery, and Exploitation of Plant Pattern Recognition Receptors for Broad-Spectrum Disease Resistance. Annual Review of Phytopathology. 55:257-286.
4. Bhandari, D.D., Lapin, D., Kracher, B., von Born, P., Bautor, J., Niefind, K., Parker, J.E. 2019. An EDS1 heterodimer signalling surface enforces timely reprogramming of immunity genes in Arabidopsis. Nature Comm. 10:772.
5. Birker, D., Heidrich, K., Takahara, H., Narusaka, M., Deslandes, L., Narusaka, Y., Reymond, M., Parker, J.E., O'Connell, R. 2009. A locus conferring resistance to Colletotrichum higginsianum is shared by four geographically distinct Arabidopsis accessions. Plant Journal. 60:602-613.
6. Century, K.S., Holub, E.B., Staskawicz, B.J. 1995. NDR1, a locus of Arabidopsis thaliana that is required for disease resistance to both a bacterial and a fungal pathogen. PNAS USA. 92:6597-6601.
7. Clough, S.J. and Bent, A.F. 1998 Floral dip: a simplified method for Agrobacterium-mediated transformation of Arabidopsis thaliana. Plant Journal. 16:735-43.

476 8. Cui, H., Tsuda, K., Parker, J.E. 2015. Effector-Triggered Immunity: From Pathogen
477 Perception to Robust Defense. Ann. Rev. of Plant Bio. 66:487-511.
478 9. Cui, H., Gobbato, E., Kracher, B., Qiu, J., Bautor, J., Parker, J.E. 2017 A core
479 function of EDS1 with PAD4 is to protect the salicylic acid defense sector in
480 Arabidopsis immunity. New Phytologist. 213:1802-1817.
481 10. Cui, H., Qiu, J., Zhou, Y., Bhandari, D.D., Zhao, C., Bautor, J., Parker, J.E. 2018.
482 Antagonism of Transcription Factor MYC2 by EDS1/PAD4 Complexes Bolsters
483 Salicylic Acid Defense in Arabidopsis Effector-Triggered Immunity. Molecular
484 Plant.11:1053-1066.
485 11. Dodds, P.N., Rathjen, J.P. 2010. Plant immunity: towards an integrated view of
486 plant-pathogen interactions. Nature Reviews Genetics.11:539-548.
487 12. Feys, B.J., Moisan, L.J., Newman, M.A., Parker, J.E. 2001. Direct interaction
488 between the Arabidopsis disease resistance signaling proteins, EDS1 and PAD4.
489 EMBO Journal. 20:5400-5411.
490 13. Feys, B.J., Wiermer, M., Bhat, R.A., Moisan, L.J., Medina-Escobar, N., Neu, C.,
491 Cabral, A., Parker, J.E. 2005. Arabidopsis SENESCENCE-ASSOCIATED
492 GENE101 stabilizes and signals within an ENHANCED DISEASE
493 SUSCEPTIBILITY1 complex in plant innate immunity. Plant Cell.17:2601-2613.
494 14. Gantner, J., Ordon, J., Kretschmer, C., Guerois, R., Stuttmann, J. 2019. An EDS1-
495 SAG101 Complex is Essential for TNL-mediated Immunity in Nicotiana
496 benthamiana. Plant Cell. pii: tpc.00099.2019
497 15. García, A.V., Blanvillain-Baufumé, S., Huibers, R.P., Wiermer, M., Li, G., Gobbato
498 E., Rietz, S., Parker, J.E. 2009. Balanced nuclear and cytoplasmic activities of
499 EDS1 are required for a complete plant innate immune response. PLoS
500 Pathogens. 6:e1000970.

16. Gehl, C., Kaufholdt, D., Hamisch, D., Bikker, R., Kudla, J., Mendel, R.R., Hänsch, R. 2011. Quantitative analysis of dynamic protein-protein interactions in planta by a floated-leaf luciferase complementation imaging (FLuCI) assay using binary Gateway vectors. Plant Journal.67:542-553.
17. Glazebrook, J., Zook, M., Mert, F., Kagan, I., Rogers, E.E., Crute, I.R., Holub, E.B., Hammerschmidt, R., Ausubel, F.M. 1997. Phytoalexin-deficient mutants of Arabidopsis reveal that PAD4 encodes a regulatory factor and that four PAD genes contribute to downy mildew resistance. Genetics.146:381-392.
18. Heidrich, K., Wirthmueller, L., Tasset, C., Pouzet, C., Deslandes, L., Parker, J.E. 2011. Arabidopsis EDS1 connects pathogen effector recognition to cell compartment-specific immune responses. Science. 334:1401-1404.
19. Jirage, D., Tootle, T.L., Reuber, T.L., Frost, L.N., Feys, B.J., Parker, J.E., Ausubel F.M., Glazebrook, J. 1999. Arabidopsis thaliana PAD4 encodes a lipase-like gene that is important for salicylic acid signaling. PNAS USA.96:13583–13588.
20. Jones, J.D., Vance, R.E., Dangl, J.L. 2016. Intracellular innate immune surveillance devices in plants and animals. Science. 354:aaf6395.
21. Jones, J.D., Dangl, J.L. 2006. The plant immune system. Nature. 16:323-329.
22. Khan, F.I., Lan, D., Durrani, R., Huan, W., Zhao, Z., Wang, Y. 2017. The Lid Domain in Lipases: Structural and Functional Determinant of Enzymatic Properties. Front. Bioeng. Biotech. 5:16.
23. Lapin, D., Kovacova, V., Sun, X., Dongus, J.A., Bhandari, D.D., von Born, P., Bautor, J., Guarneri, N., Stuttmann, J., Beyer, A., Parker, J.E. 2019. A coevolved EDS1-SAG101-NRG1 module mediates cell death signaling by TIR-domain immune receptors. BioRxiv: doi: https://doi.org/10.1101/572826

525 24. Louis, J., Gobbato, E., Mondal, H.A., Feys, B.J., Parker, J.E., Shah, J. 2012.
526 Discrimination of Arabidopsis PAD4 Activities in Defense against Green Peach
527 Aphid and Pathogens. Plant Physiology. 158:1860-1872.
528 25. Milligan, S.B., Bodeau, J., Yaghoobi, J., Kaloshian, I., Zabel, P., and Williamson,
529 V.M. 1998. The Root Knot Nematode Resistance Gene Mi from Tomato Is a
530 Member of the Leucine Zipper, Nucleotide Binding, Leucine-Rich Repeat Family of
531 Plant Genes. Plant Cell. 10:1307.
532 26. Mindrebo, J.T., Nartey, C.M., Seto, Y., Burkart, M.D., Noel, J.P. 2016. Unveiling
533 the functional diversity of the alpha/beta hydrolase superfamily in the plant
534 kingdom. Current Opinion Struct. Biology. 41:233-246.
535 27. Mine, A., Nobori, T., Salazar-Rondon, M.C. Winkelmüller, T.M., Anver, S., Becker,
536 D., Tsuda, K. 2017. An incoherent feed-forward loop mediates robustness and
537 tunability in a plant immune network. EMBO Reports.18:464-476.
538 28. Murase, K., Hirano, Y., Sun, T.P., Hakoshima, T. 2008. Gibberellin-induced DELLA
539 recognition by the gibberellin receptor GID1. Nature. 456:459-463.
540 29. Muskett, P.R., Kahn, K., Austin, M.J., Moisan, L.J., Sadanandom, A., Shirasu, K.,
541 Jones, J.D.G., Parker, J.E. 2002. Arabidopsis RAR1 Exerts Rate-Limiting Control
542 of R Gene-Mediated Defenses against Multiple Pathogens. Plant Cell. 14:979-992.
543 30. Nalam, V., Louis, J., Patel, M. and Shah, J. 2018. Arabidopsis-Green Peach Aphid
544 Interaction: Rearing the Insect, No-choice and Fecundity Assays, and Electrical
545 Penetration Graph Technique to Study Insect Feeding Behavior. Bio-protocol
546 8(15): e2950.
547 31. Narusaka, M., Shirasu, K. Noutoshi, Y., Kubo, Y., Shiraishi, T., Iwabuchi, M.,
548 Narusaka, Y. 2009.. RRS1 and RPS4 provide a dual resistance-gene system
549 against fungal and bacterial pathogens. Plant Journal. 60:218-226.

550 32. Rossi, M., Goggin, F.L., Milligan, S.B., Kaloshian, I., Ullman, D.E., Williamson,
551 V.M. 1998. The nematode resistance gene Mi of tomato confers resistance against
552 the potato aphid. PNAS USA. 95:9750-9754.
553 33. Parker, J.E., Holub, E.B., Frost, L.N., Falk, A., Gunn, N.D., Daniels, M.J. 1996.
554 Characterization of eds1, a mutation in Arabidopsis suppressing resistance to
555 Peronospora parasitica specified by several different RPP genes. Plant Cell.
556 8:2033-2046.
557 34. Pegadaraju, V., Knepper, C., Reese, J., Shah, J. 2005. Premature leaf senescence
558 modulated by the Arabidopsis PHYTOALEXIN DEFICIENT4 gene is associated
559 with defense against the phloem-feeding green peach aphid. Plant Physiology.
560 139:1927-1934.
561 35. Pegadaraju, V., Louis, J., Singh, V., Reese, J.C., Bautor, J., Feys, B.J., Cook, G.,
562 Parker, J.E., Shah, J. 2007. Phloem-based resistance to green peach aphid is
563 controlled by Arabidopsis PHYTOALEXIN DEFICIENT4 without its signaling
564 partner ENHANCED DISEASE SUSCEPTIBILITY1. Plant Journal. 52:332-341.
565 36. Rauwerdink, A., and Kazlauskas, R. J. 2015. How the Same Core Catalytic
566 Machinery Catalyzes 17 Different Reactions: the Serine-Histidine-Aspartate
567 Catalytic Triad of α/β-Hydrolase Fold Enzymes. ACS Catalysis. 5:6153-6176.
568 37. Rietz, S., Stamm, A., Malonek, S., Wagner, S., Becker, D., Medina-Escobar, N.,
569 Vlot, A.C., Feys, B.J., Niefind, K., Parker, J.E. 2011. Different roles of Enhanced
570 Disease Susceptibility1 (EDS1) bound to and dissociated from Phytoalexin
571 Deficient4 (PAD4) in Arabidopsis immunity. New Phytologist. 191:107-119.
572 38. Saucet, S.B., Ma, Y., Sarris, P.F., Furzer, O.J., Sohn, K.H., Jones, J.D. 2015. Two
573 linked pairs of Arabidopsis TNL resistance genes independently confer recognition
574 of bacterial effector AvrRps4. Nature Comm. 6:6338.

575 39. Shimada, A., Ueguchi-Tanaka, M., Nakatsu, T., Nakajima, M., Naoe, Y., Ohmiya,
576 H., Kato, H., Matsuoka, M. 2008. Structural basis for gibberellin recognition by its
577 receptor GID1. Nature. 456:520-523.
578 40. Stuttmann, J., Peine, N., Garcia, A.V., Wagner, C., Choudhury, S.R., Wang, Y.,
579 James, G.V., Griebel, T., Alcázar, R., Tsuda, K., Schneeberger, K., Parker, J.E.
580 2016. Arabidopsis thaliana DM2h (R8) within the Landsberg RPP1-like Resistance
581 Locus Underlies Three Different Cases of EDS1-Conditioned Autoimmunity. PLoS
582 Genetics 12:e1005990.
583 41. Van der Biezen, E.A., Freddie, C.T., Kahn, K., Parker, J.E., Jones, J.D. 2002.
584 Arabidopsis RPP4 is a member of the RPP5 multigene family of TIR-NB-LRR
585 genes and confers downy mildew resistance through multiple signalling
586 components. Plant Journal. 29:439-451.
587 42. Villada, E.S., González, E.G., López-Sesé, A.I., Castiel, A.F., Gómez-Guillamón,
588 M.L. 2009. Hypersensitive response to Aphis gossypii Glover in melon genotypes
589 carrying the Vat gene. Journal of Experimental Botany. 60:3269-3277.
590 43. Wagner, S., Stuttmann, J., Rietz, S., Guerois, R., Brunstein, E., Bautor, J., Niefind,
591 K., Parker, J.E. 2013. Structural basis for signaling by exclusive EDS1 heteromeric
592 complexes with SAG101 or PAD4 in plant innate immunity. Cell Host
593 Microbe.14:619-630.
594 44. Wang, D., Zhang, L., Hu, J., Gao, D., Liu, X., Sha, Y. 2018. Comparative genomic
595 analysis of the Lipase3 gene family in five plant species reveals distinct
596 evolutionary origins. Genetica.146:179-185.
597 45. Witte, C.-P., Noël, L., Gielbert, J., Parker, J., Romeis, T. 2004. Rapid one-step
598 protein purification from plant material using the eight-amino acid StrepII epitope.
599 Plant Molecular Biology. 55:135-147.

600 46. Wroblewski, T., Piskurewicz, U., Tomczak, A., Ochoa, O., Michelmore, R.W. 2007.
601 Silencing of the major family of NBS-LRR encoding genes in lettuce results in the
602 loss of multiple resistance specificities. Plant Journal. 51:803-818
603 47. Zhou, N., Tootle, T.L., Tsui, F., Klessig, D.F., Glazebrook J. 1998. PAD4 functions
604 upstream from salicylic acid to control defense responses in Arabidopsis. Plant
605 Cell. 10:1021-1030.

606

607 **Supplemental Material**

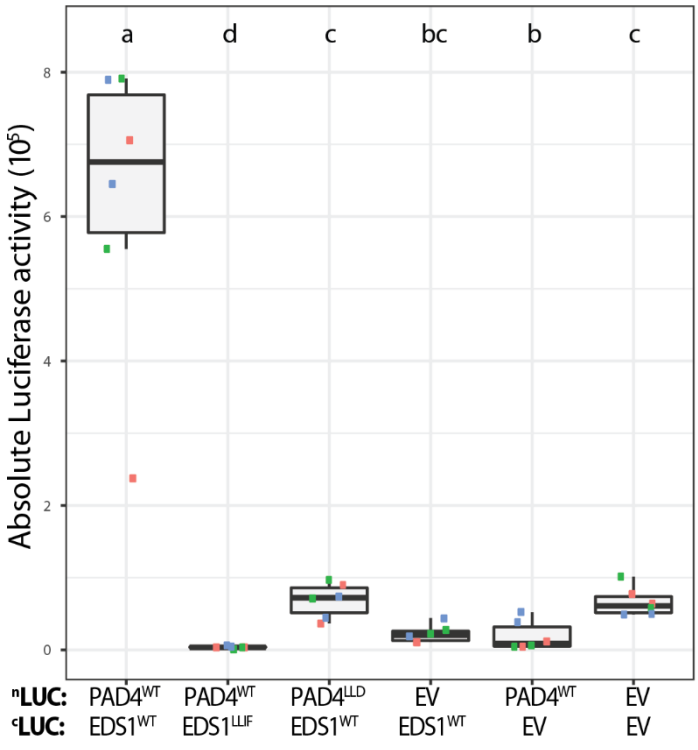

608

609 **Figure S1. Split-luciferase interaction assay**

610 Absolute luciferase (LUC) activity from transiently co-expressed N-LUC or C-LUC
611 constructs (35S promoter) in *N. benthamiana*. Data are pooled from three independent
612 experiments with two biological replicates per experiment (n = 6). Error bars = SEM.
613 Letters indicate statistical significance as determined by one-way ANOVA with multiple
614 testing correction using Tukey-HSD; $p < 0.01$.

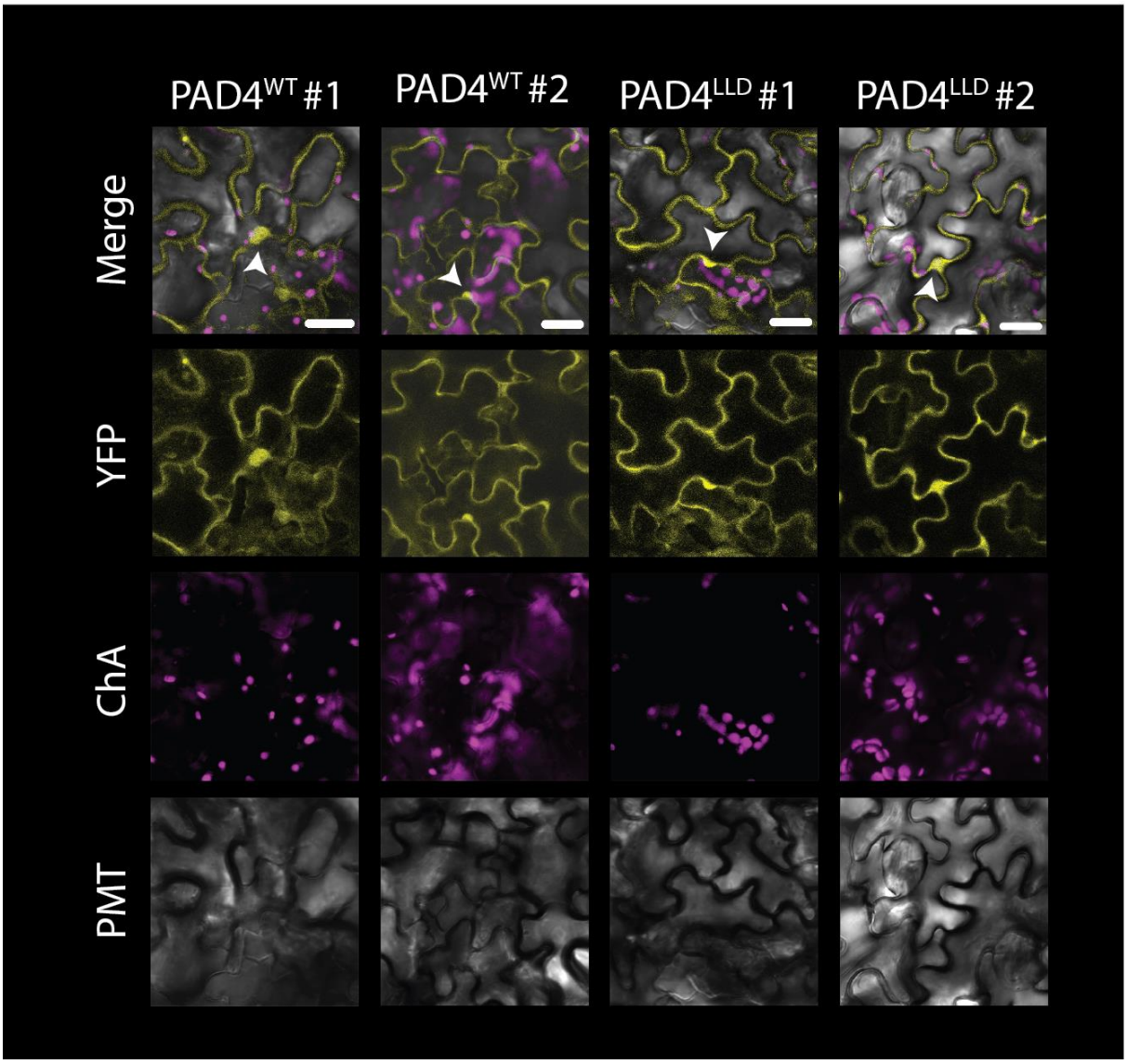

Figure S2. PAD4 localization at 24 hpi with *Pst* AvrRps4

Nucleocytoplasmic localization of YFP-PAD4^{WT} and YFP-PAD4^{LLD} in Arabidopsis transgenic lines (24 hpi, *Pst avrRps4*). To determine PAD4^{LLD} localizations, confocal microscope sensitivity was enhanced to enable its detection. White arrowheads indicate nuclei and white bars correspond to 20 µm. Similar results were obtained in two independent replicates in two biological replicates (n=4).

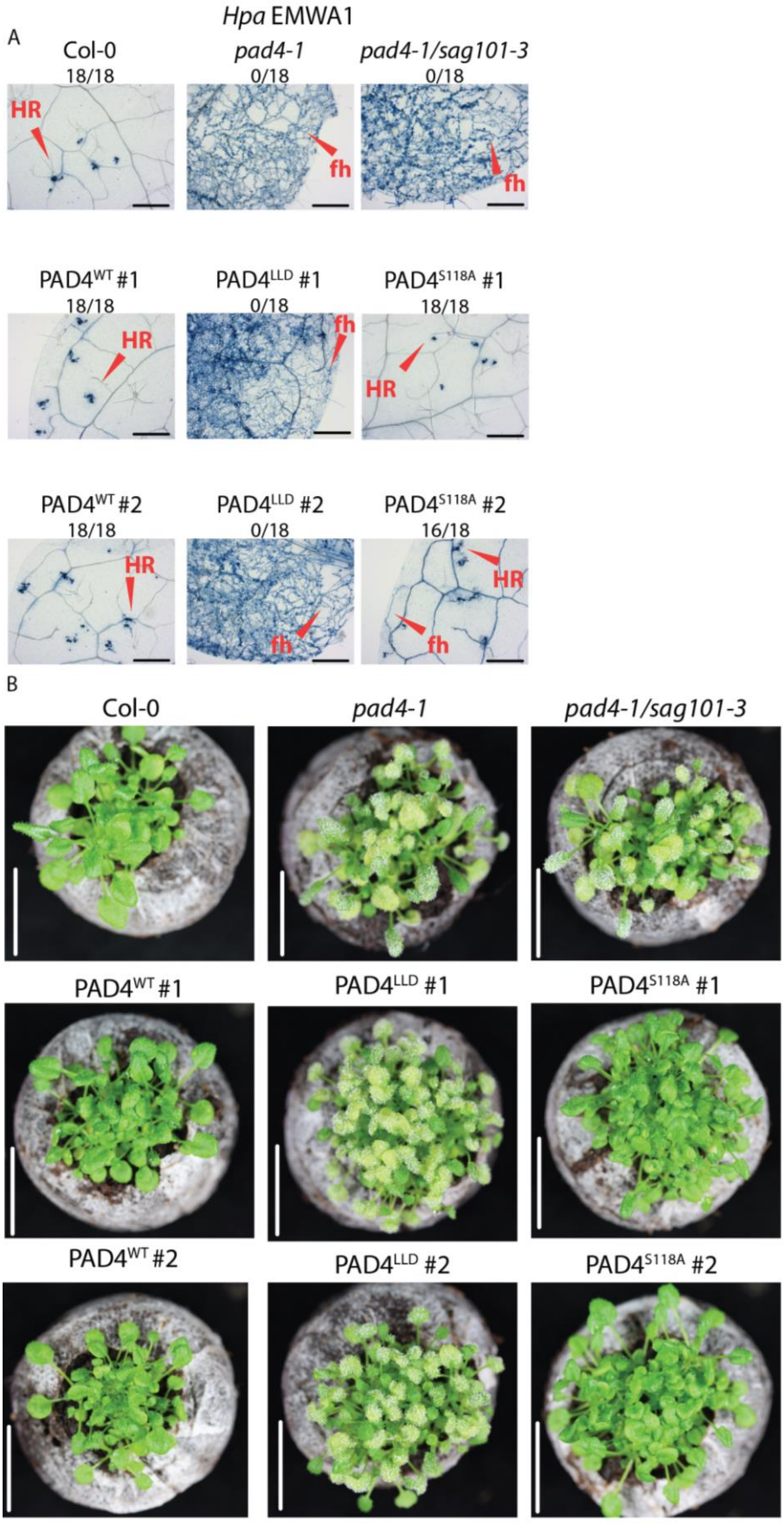

622

Figure S3. Microscopic and macroscopic disease phenotypes of *Hpa* EMWA1-infected Arabidopsis plants

A. Microscopic immunity phenotypes of 3-week-old Arabidopsis lines, as indicated, at 6 dpi with *Hpa* isolate EMWA1 (recognized by TNL RPP4). Trypan blue-stained leaves showing free hyphae (fh) and hypersensitive cell death (Hypersensitive Response (HR)). Black bars represent 500 µm. Fractions (*e.g.* 18/18) indicate numbers of resistant leaves/total plants tested. Pictures are representative from three independent experimental replicates, > 6 leaves per replicate and > 30 infection sites per genotype. **B.** *Hpa* EMWA1-inoculated plants of the same lines as in A. Resistant plants look healthy at 6 dpi, whereas susceptible plants produce conidiospores and leaf chlorosis. White bars correspond to 2 cm.

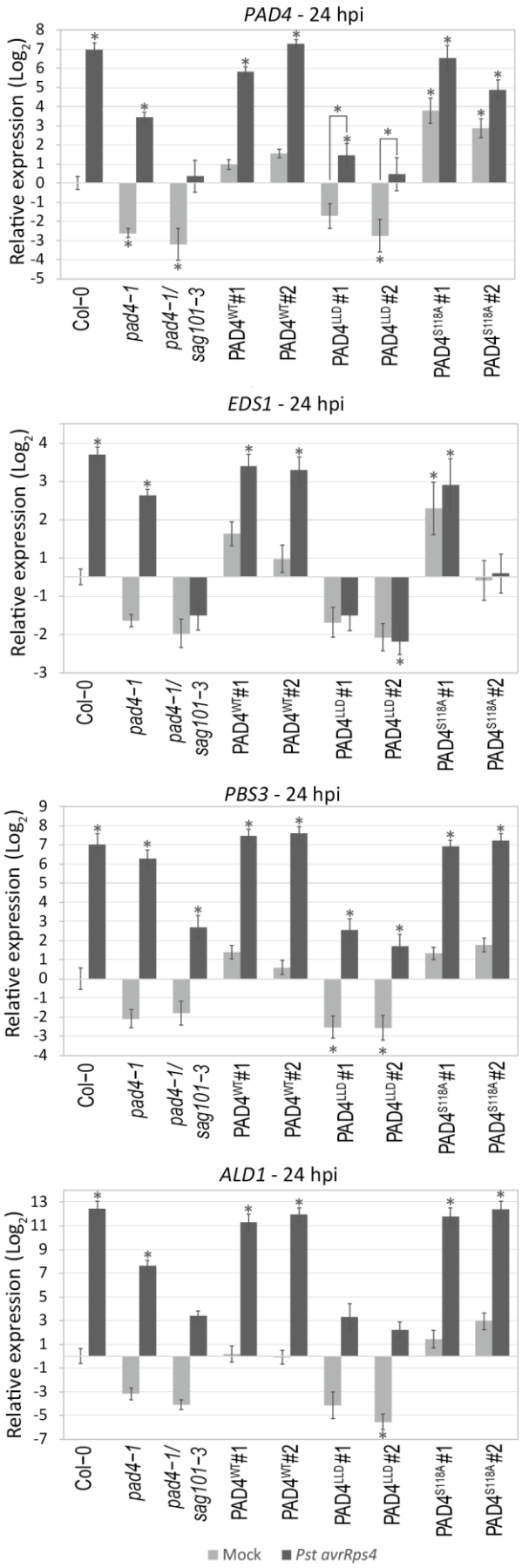

Figure S4. Relative expression of *EDS1*-dependent defense marker genes

Transcript abundance was determined by RT-qPCR in 4-week old Arabidopsis plants of the indicated lines syringe infiltrated with buffer- (mock, grey bars) or *Pst avrRps4* (black bars) (24 hpi). Data are pooled from three independent experiments with two to three biological replicates per experiment (n = 6-9). Transcript abundances of *PAD4, EDS1, AVRPPHB SUSCEPTIBLE 3* (*PBS3*) and *GD2-LIKE DEFENSE RESPONSE PROTEIN 1* (*ALD1*) were measured relative to *ACT2*. Relative expression and significance level are set to Col-0 mock-treated samples. Bars represent mean of three experimental replicates ± SE. Differences between genotypes were determined by using ANOVA (Tukey-HSD, p <0.01), letters indicate significance class and asterisk indicates $p < 0.01$.

646 **Table S1. List of DNA primers used in this study**

Purpose	Primer	Oligo Sequence
Cloning	PAD4_LLD_F	CCTATTCTGAGGTAAGCTGAGTTAGCC
Cloning	PAD4_LLD_R	GGCTAACTCAGCTTACCTCAGAATAGG
qPCR	qPAD4_F	GGTTCTGTTCGTCTGATGTTT
qPCR	qPAD4_R	GTTCCTCGGTGTTTTGAGTT
qPCR	qEDS1_F	CGAAGACACAGGGCCGTA
qPCR	qEDS1_R	AAGCATGATCCGCACTCG
qPCR	qPBS3_F	ACACCAGCCCTGATGAAGTC
qPCR	qPBS3_R	CCCAAGTCTGTGACCCAGTT
qPCR	qICS1_F	TTCTGGGCTCAAACACTAAAAC
qPCR	qICS1_R	GGCGTCTTGAAATCTCCATC
qPCR	qFMO1_F	GTTCGTGGTTGTGTGTACCG
qPCR	qFMO1_R	TGTGCAAGCTTTTCCTCCTT
qPCR	qPR1_F	TTCTTCCCTCGAAAGCTCAA
qPCR	qPR1_R	AAGGCCCACCAGAGTGTATG
qPCR	qALD1_F	TGGCCTTAAGGAGATACGGT
qPCR	qALD1_R	ACCTGAGCCTGGTACTGTTA
Genotyping	pad4-1_F	GCGATGCATCAGAAGAG
Genotyping	pad4-1_R	TTAGCCCAAAAGCAAGTATC
Genotyping	SAG101_F	GCGGCCTCCTCTCTACTTCT
Genotyping	SAG101_R	CTTCTTGAAACCATCGAACC
Genotyping	sag101-3_F (GABI-KAT)	ATATTGACCATCATACTCATTGC
Genotyping	sag101-3_R	TTGTGACTTACCATAACTCTCG
Genotyping	EDS1_F	ACACAAGGGTGATGCGAGACA
Genotyping	eds1-2_F	CAAACGTCAAGAGAGCTGAG
Genotyping	eds1-2/EDS1_R	GTGGAAACCAAATTTGACATTAG

647